



Two-step photoionization of *trans*-stilbene in acetonitrile via an ion-pair precursor studied with picosecond time-resolved absorption and Raman spectroscopies

Hiroko Miki^a, Kyouosuke Yoshida^a, Chieko Kawate^a, Rintaro Shimada^a, Tomohisa Takaya^b, Koichi Iwata^b, Hiro-o Hamaguchi^{a,c,*}

^a Department of Chemistry, School of Science, The University of Tokyo, 7-3-1 Hongo, Bunkyo-ku, Tokyo 113-0033, Japan

^b Department of Chemistry, Faculty of Science, Gakushuin University, 1-5-1 Mejiro, Toshima-ku, Tokyo 171-8588, Japan

^c Institute of Molecular Science and Department of Applied Chemistry, National Chiao Tung University, 1001 Ta Hsueh Road, Hsinchu, Taiwan

ARTICLE INFO

Article history:

Received 26 October 2011

In final form 30 December 2011

Available online 5 January 2012

ABSTRACT

Picosecond time-resolved visible absorption and Raman spectra of *trans*-stilbene in acetonitrile have been measured. A new transient absorption band is observed at 440 nm, whose decay time constant coincides with that of the rise of the radical cation. In addition to the known Raman bands of the radical cation, a new Raman feature showing a fast decay is found at 1599 cm⁻¹. We assign the 440 nm absorption band and the 1599 cm⁻¹ Raman band to a precursor of the radical cation. The precursor may well be an ion pair that holds an ejected electron still around the cation.

© 2012 Elsevier B.V. All rights reserved.

1. Introduction

Photo-induced dynamics of organic molecules in solution has been studied extensively as the most fundamental and elementary physicochemical process that is well suited to trace with ultrafast time-resolved spectroscopy. *Trans*-stilbene is a prototype organic molecule that shows many interesting photo-induced dynamics [1]. The lowest excited singlet state (*S*₁) of *trans*-stilbene has been studied intensively as the key intermediate of the *trans*-*cis* photoisomerization. Time-resolved visible absorption [2–4], Raman [5–16] and infrared [17,18] spectroscopies have shed considerable lights on the structure and dynamics of *S*₁ *trans*-stilbene and the 'solvent-induced dynamic polarization' model of photoisomerization has been proposed [5,19].

It is also known that photoionization of *trans*-stilbene occurs in solution to generate the *trans*-stilbene radical cation. The ionization mechanism still remains controversial with an intriguing fact that the rise of the radical cation shows a marked delay from the photoexcitation [3,20]; picosecond time-resolved Raman spectroscopy gives a rise time constant of 17 ps in acetonitrile [20]. From the viewpoint of energetics, two-photon ionization is the most probable. Since the ionization energy of *trans*-stilbene in the gas phase is 7.656 eV [21], the one-photon energy of ultraviolet (260–300 nm, 4.77–4.13 eV) light is not enough but the two-photon energy (9.54–8.27 eV) is large enough for ionization. In fact, two-photon ionization mechanism has been suggested from the

photoexcitation laser power dependence of the cation formation by picosecond time-resolved Raman [20] and nanosecond absorption [22] spectroscopies. Two-photon absorption is an instantaneous optical process and, if photoionization takes place directly from the two-photon excited state, it should occur without any time delay. A new mechanism that involves both two-photon excitation and intermediate formation is necessary to fully account for these previous findings.

In the present Letter, we study picosecond time-resolved visible absorption and Raman spectra of *trans*-stilbene in acetonitrile. The structure and dynamics of a newly found transient species, which is found to exist just after the photoexcitation and which we identify as a precursor of the *trans*-stilbene radical cation, are discussed. Absorption spectroscopy determines the dynamics of this species precisely, while Raman helps us to elucidate its structure with reference to the known Raman spectra of *S*₁ *trans*-stilbene [5,14] and those of the *trans*-stilbene radical cation [23].

2. Experimental

Sub-picosecond time-resolved visible absorption spectra were measured with a laboratory constructed pump-probe time-resolved ultraviolet-visible absorption spectroscopic system. The output of a regenerative amplified mode-locked Ti:sapphire laser (Legend Elite USP-HE, Coherent, 800 nm, 1 kHz, 3.4 mJ) was divided into two. One beam was introduced to an optical parametric amplifier (OPA, TOPAS-C, Light Conversion) to generate the pump light at 297 nm. The other was focused onto a CaF₂ plate to obtain broadband probe light (370–750 nm) by self phase modulation.

* Corresponding author. Fax: +81 3 3818 4621.

E-mail address: hhama@chem.s.u-tokyo.ac.jp (H. Hamaguchi).

A small portion of the probe light was separated and used as the reference light. After passing through an optical delay line, the probe and pump beams were focused onto a flowing jet film of the sample solution. The transmitted probe light and the reference light were dispersed by a spectrometer and detected by a liquid-nitrogen cooled CCD detector (Spec-10: 400B/LN, Princeton Instruments). Pump power at the sample point was ~ 1.2 mW. The polarizations of the pump and probe beams were set to make the magic angle (54.7°). Instrumental response time was ~ 180 fs.

Picosecond time-resolved Raman spectra were measured with a laboratory constructed Raman spectroscopic system. A regenerative/multi-pass amplified mode-locked Ti:sapphire laser (Integra, Quantronix, 800 nm, 1 kHz, 2 mJ) pumped two OPAs (TOPAS, Quantronix) to obtain the pump (300 nm, ~ 1 mW at sample) and probe (455 nm, ~ 0.1 mW at sample) light beams. Bandwidth of the probe light was narrowed by a grating-slit bandpass filter. The pump beam was introduced to an optical delay line before reaching the sample. The pump and probe beams were focused with $f = 75$ mm and $f = 50$ mm lenses, respectively, and superimposed from opposite directions on a flowing jet film of the sample solution. The 90° scattered Raman light was collected and dispersed by a spectrometer (HR-320, Horiba Jobin Yvon), and detected by a liquid-nitrogen cooled CCD detector (Spec 10:400B/LN, Princeton Instruments). Rayleigh scattering was eliminated by a notch filter (Iridian) placed in front of the entrance slit of the spectrometer. The temporal resolution of the instrument was 6 ps. The integration time at one time delay was 15 s and 27 series of measurements with randomized time delays were performed and summed up.

The sample of *trans*-stilbene (special grade) and solvent acetonitrile (HPLC Grade) were purchased from Wako Pure Chemical Industries and used as received. The concentration of *trans*-stilbene was 3 mM for all measurements. All the measurements were performed at room temperature.

3. Results and discussion

3.1. Picosecond time-resolved visible absorption spectra

Picosecond time-resolved visible absorption spectra of *trans*-stilbene in acetonitrile are shown in Figure 1. Strong transient absorption bands are observed at 580 and 470 nm. They are known

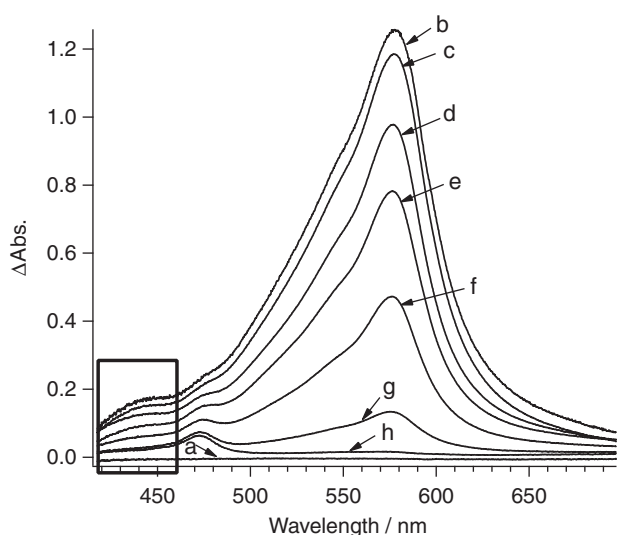


Figure 1. Picosecond time-resolved visible absorption spectra of *trans*-stilbene in acetonitrile measured at delay times (a) -1 ps, (b) 6 ps, (c) 10 ps, (d) 20 ps, (e) 30 ps, (f) 50 ps, (g) 100 ps and (h) 250 ps. Absorption bands surrounded by a rectangle is the new absorption band at 440 nm.

to arise from S_1 *trans*-stilbene [2] and the *trans*-stilbene radical cation [3,23], respectively. In addition to these well-known bands, we find a new feature around 440 nm (the rectangle in Figure 1). Time-dependence plots of these three absorption bands are shown in Figure 2. The S_1 intensity is obtained by integration of the absorption from 490 to 700 nm. The intensities of the radical cation and the newly found band are obtained after subtracting the contribution of the S_1 absorption approximated by combined Gaussian functions. Figure 2 clearly shows an instantaneous rise of the S_1 absorption band (Figure 2c) and a delayed rise of the radical cation absorption (Figure 2b). The newly found absorption band also rises instantaneously within the instrumental function of the apparatus and decays in tens of picoseconds (Figure 2a). Exponential fits of the obtained time profiles give the lifetime of the S_1 state as 40 ps and the rise time of the radical cation as 38 ps. Those numbers are consistent with the already reported literature values [3]. The decay time of the newly found band at 440 nm is obtained as 46 ps. The agreement of this time constant with those of the S_1 decay and the radical cation rise implies the following two possibilities for the assignment of the 440 nm band. The first possibility is that it is assigned to a higher $S_n \leftarrow S_1$ transition arising from the S_1 state. The second is that it is ascribed neither to the S_1 state nor to the radical cation but to a precursor of the radical cation. As far as the authors are aware, the transient absorption at 440 nm and hence the transient species giving rise to this band have never been reported in the literature. Raman excitation close to 440 nm is expected to resonantly enhance the bands due to this transient and give a clue to its identification (see the following discussion of the 455 nm excited Raman spectra).

3.2. Picosecond time-resolved Raman spectra

Picosecond time-resolved Raman spectra of *trans*-stilbene in acetonitrile measured with 455 nm excitation are shown in Figure 3. At early delay times until 1 ps, the Raman spectra show bands at 1599 , 1529 , 1286 and 1161 cm^{-1} . The 1529 and 1161 cm^{-1} bands decay in tens of picoseconds, while the 1599 and 1286 cm^{-1} bands show increases in intensities. The band at 1599 cm^{-1} shifts to higher wavenumbers with increasing delay time and eventually reaches 1609 cm^{-1} at 1000 ps. The width of this 1599 cm^{-1} band becomes smaller with increasing delay time. At later delay times, several more bands appear and the spectra eventually have bands at 1609 , 1349 , 1291 , 1207 , 1162 , 994 and 866 cm^{-1} .

The Raman bands at 1529 and 1161 cm^{-1} correspond well to those of the S_1 state observed with 577 nm excitation [14]. We assign these bands to the S_1 state. This assignment is consistent with the observed decay behaviors of the two bands. The spectra observed after 98 ps agree well with those of the *trans*-stilbene radical cation excited at 480 nm [23]. We note that the band at 1207 cm^{-1} has not been reported in the literature, though it shows a time evolution similar to the other radical cation bands. The intensities of the S_1 bands are much lower than those of the radical cation bands, indicating that they are not resonance enhanced with 455 nm excitation. Therefore, the S_1 state is not likely to be the origin of the 440 nm absorption, leaving the possibility of the assignment to a precursor of the radical cation.

Apart from the extra bands due to the S_1 state at 1529 and 1161 cm^{-1} , the 1 ps spectrum shows a small but significant deviation from the radical cation spectrum observed after 98 ps. The peak position of the 1599 cm^{-1} band is 10 cm^{-1} lower than the corresponding band (1609 cm^{-1}) of the radical cation. This deviation indicates that the 1 ps Raman spectrum is contributed dominantly by the precursor of the radical cation. In order to confirm this assignment, the time dependence of the intensity of the $1599/1609$ cm^{-1} band is examined. Because significant overlap of

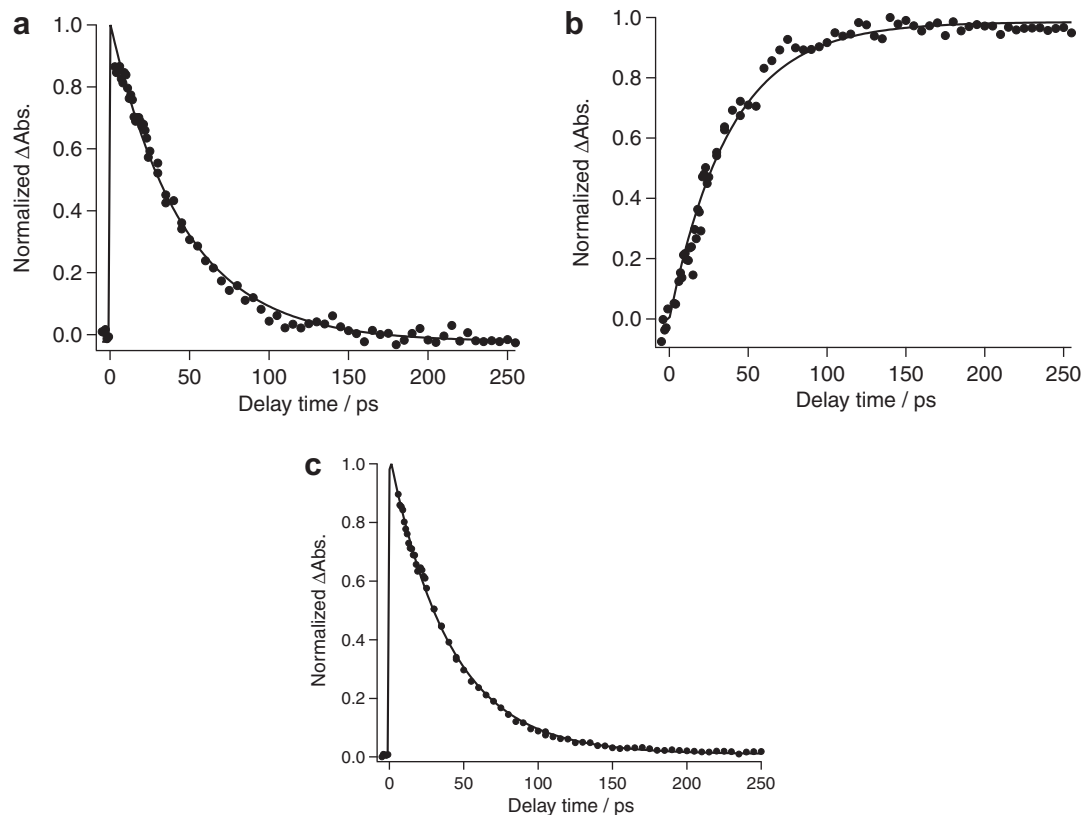


Figure 2. Time dependence of (a) the newly found absorption at 440 nm, (b) the radical cation and (c) the S_1 state. Full lines show least-squares fitted exponential functions.

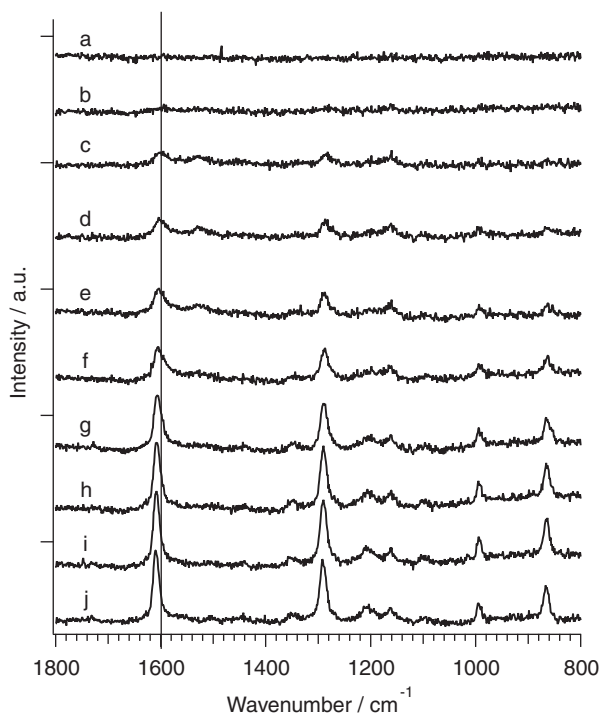


Figure 3. Picosecond time-resolved Raman spectra of *trans*-stilbene in acetonitrile measured at delay times of (a) -5 ps, (b) -2 ps, (c) 1 ps, (d) 3 ps, (e) 8 ps, (f) 18 ps, (g) 38 ps, (h) 58 ps, (i) 98 ps and (j) 1000 ps.

the two bands occurs in the delay times larger than 1 ps with appreciable peak shifts, the integrated intensity between 1560 and 1656 cm^{-1} is used for the analysis. This integrated intensity

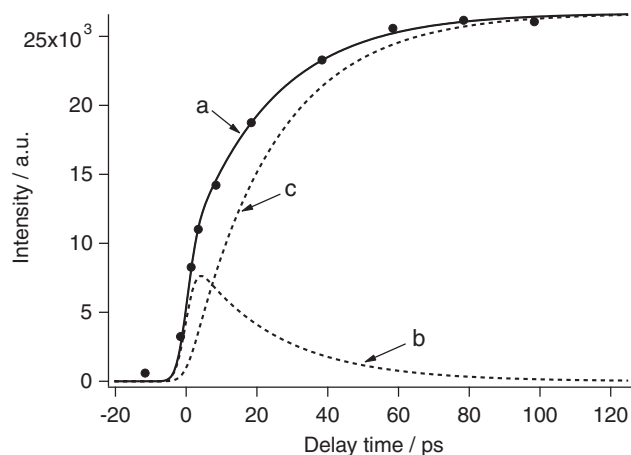


Figure 4. Time dependence of the integrated Raman intensity in the 1560 and 1656 cm^{-1} region (filled circles). The full line (a) indicates the least-squares fitted exponential function, $A_1 \exp(-t/\tau) + A_2 \{1 - \exp(-t/\tau)\}$ with $A_1 = 27000$, $A_2 = 9500$, $\tau = 24$ ps. The dotted lines (b) and (c) show the two components $A_1 \exp(-t/\tau)$ and $A_2 \{1 - \exp(-t/\tau)\}$, respectively, with $A_1 = 27000$, $A_2 = 9500$, $\tau = 24$ ps. The two exponential functions are convoluted with the instrumental function represented by a Gaussian with full-width-half-maximum of 5.5 ps (see text).

is expected to have contributions from two components; one corresponds to the precursor that shows an instantaneous rise followed by a decay and the other corresponds to the radical cation that shows a rise with a time constant equal to the decay of the precursor. Figure 4 shows the time dependence of the integrated intensity of the 1599/1609 cm^{-1} band. This time dependence can not be fitted with a single exponential function; the intensities before 1 ps are too large to be fitted with a single exponential rise.

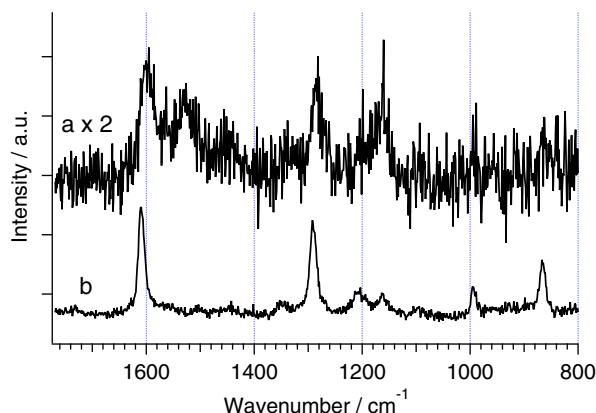


Figure 5. Raman spectra of (a) the ion-pair precursor plus the S_1 state and (b) the radical cation.

Rather, fitting with a linear combination of two components, one with an instantaneous rise and a 24 ps exponential decay and the other with a 24 ps exponential rise, reproduce the observed curve very well (full line in Figure 4). This fitting analysis indicates that the contribution of the radical cation bands to the 1 ps Raman spectrum is only 10%. It is thus confirmed that the 1 ps Raman spectrum is dominated by the bands due to the precursor of the radical cation.

In order to extract genuine Raman spectrum of the precursor, we subtract out the contribution of the radical cation from the 1 ps Raman spectrum using the coefficient 0.04 obtained from the fitting analysis in Figure 4. The result is shown in Figure 5 in comparison with that of the radical cation observed at 1000 ps. Except for the two S_1 Raman bands at 1529 and 1161 cm^{-1} , the two Raman spectra resemble each other. Corresponding to the radical cation peaks at 1609, 1349, 1291, 1207, 1162, 994 and 866 cm^{-1} , the precursor spectrum shows similar but appreciably broader peaks at 1599 and 1285 cm^{-1} . The general resemblance of the two Raman spectra indicates that the precursor has a structure very similar to that of the radical cation and that it is most probably a cationic species that has an electron already ejected.

With excitation at 300 nm, an electron in the ground electronic state is two-photon excited to a state higher in energy than the ionization threshold. This high-energy two-photon excited state is expected to be very short-lived and eject an electron immediately to produce an ion pair. First, a contact ion pair [24,25] is formed and it is eventually solvated to generate a free radical cation and a solvated electron. A solvent-separated ion pair [24,25] may also be involved. The ion pair is formed with some excess energy (hot ion pair) and subsequently dissipates thermal energy to the surrounding solvent molecules. Thus, the first tens of picoseconds in the present experiments are looking at the solvation/cooling process of the hot ion pair and the formation of the free radical ion therefrom. The precursor Raman spectrum in Figure 5 is ascribed to hot ion pair species (contact or solvent-separated). The

hot free radical cation is not a primary contributor to the 1 ps spectrum, because the 440 nm absorption is totally different from the free radical cation absorption. Note that thermally hot species generally show electronic absorption spectra broader than but similar to the room-temperature spectra. On the other hand, spectral shifts of several tens of nm between the contact ion pair and the free ion are known to support the present assignment [26,27]. Solvated electrons exhibit broad absorption bands in the wavelength range >700 nm [28]. Due to the limitation of the spectral coverage, their formation dynamics have not been clarified in the present experiment.

In conclusion, we assign the newly found 440 nm transient absorption band and the 1599 cm^{-1} Raman band to the precursor of the *trans*-stilbene radical cation, which is most likely to have an ion-pair structure. A two-step photoionization mechanism via an ion-pair precursor has thus been proposed for *trans*-stilbene. These findings are significant not only for understanding the photoionization of *trans*-stilbene but also for elucidating the general roles of ion pairs, contact or solvent-separated and hot or cool, in the ionization process of organic molecules in solution.

References

- [1] H. Hamaguchi, in: J.R. Durig (Ed.), *Vibrational Spectra and Structure*, vol. 16, Elsevier, 1987, p. 227 (Chapter 4).
- [2] F.E. Doany, B.I. Greene, R.M. Hochstrasser, *Chem. Phys. Lett.* 75 (1980) 206.
- [3] J. Oberlé, E. Abraham, A. Ivanov, G. Jonusauskas, C. Rullière, *J. Phys. Chem.* 100 (1996) 10179.
- [4] S.A. Kovalenko, R. Schanz, H. Hennig, N.P. Ernsting, *J. Chem. Phys.* 115 (2001) 3256.
- [5] H. Hamaguchi, K. Iwata, *Bull. Chem. Soc. Jpn.* 75 (2002) 883.
- [6] J.B. Hopkins, P.M. Renzepis, *Chem. Phys. Lett.* 124 (1986) 79.
- [7] S.A. Payne, R.M. Hochstrasser, *J. Phys. Chem.* 90 (1986) 2068.
- [8] T.L. Gustafson, D.M. Roberts, D.A. Chernoff, *J. Chem. Phys.* 79 (1983) 1559.
- [9] H. Hamaguchi, C. Kato, M. Tasumi, *Chem. Phys. Lett.* 100 (1983) 3.
- [10] H. Hamaguchi, *Chem. Phys. Lett.* 126 (1986) 185.
- [11] H. Hamaguchi, T. Urano, M. Tasumi, *Chem. Phys. Lett.* 106 (1984) 153.
- [12] T.L. Gustafson, D.M. Roberts, D.A. Chernoff, *J. Chem. Phys.* 81 (1984) 3439.
- [13] K. Iwata, H. Hamaguchi, *Chem. Phys. Lett.* 196 (1992) 462.
- [14] W.L. Weaver, L.A. Huston, K. Iwata, T.L. Gustafson, *J. Phys. Chem.* 96 (1992) 8956.
- [15] R.E. Hester, P. Matousek, J.N. Moore, A.W. Parker, W.T. Toner, M. Towrie, *Chem. Phys. Lett.* 208 (1993) 471.
- [16] K. Iwata, H. Hamaguchi, *J. Phys. Chem. A* 101 (1997) 632.
- [17] H. Okamoto, *Chem. Lett.* 27 (1998) 1141.
- [18] H. Okamoto, *J. Phys. Chem. A* 103 (1999) 5852.
- [19] K. Iwata, R. Ozawa, H. Hamaguchi, *J. Phys. Chem. A* 106 (2002) 3614.
- [20] T. Nakabayashi, S. Kamo, H. Sakuragi, N. Nishi, *J. Phys. Chem. A* 105 (2001) 8605.
- [21] W.M. Haynes (Ed.), *CRC Handbook of Chemistry and Physics*, CRC Press, 2011, 92nd ed., CRC Press, Boca Raton, FL, 2011.
- [22] M. Hara, S. Tojo, T. Majima, *J. Photochem. Photobiol. A: Chem.* 162 (2004) 121.
- [23] W. Hub, U. Klüter, S. Schneider, F. Doerr, J.D. Oxman, F.D. Lewis, *J. Phys. Chem.* 88 (1984) 2308.
- [24] W. Hub, S. Schneider, F. Dörr, J.T. Simpson, J.D. Oxman, F.D. Lewis, *J. Am. Chem. Soc.* 104 (1982) 2044.
- [25] W. Hub, S. Schneider, F. Dörr, J.D. Oxman, F.D. Lewis, *J. Am. Chem. Soc.* 106 (1984) 708.
- [26] G.G. Gurzadyan, J. Reynisson, S. Steenken, *Phys. Chem. Chem. Phys.* 9 (2007) 288.
- [27] Y. Yamamoto, S. Nishida, X.-H. Ma, K. Hayashi, *J. Phys. Chem.* 90 (1986) 1921.
- [28] A. Singh, H.D. Gesser, A.R. Scott, *Chem. Phys. Lett.* 2 (1968) 271.